# Optimal Scheduling of Commercial Demand Response by Technical Virtual Power Plants

Matthew Gough
*FEUP* and *INESC TEC*
Porto, Portugal
mattgough23@gmail.com

Sérgio F. Santos
*INESC TEC and Portucalense University Infante D. Henrique*
Porto, Portugal
sdfsantos@gmail.com

João M. B. A. Matos
*FEUP*
Porto, Portugal
joaobicomatos97@gmail.com

Juan M. Home-Ortiz
*UNESP*
Ilha Solteira, Brazil
juan.home@unesp.br

Mohammad S. Javadi
*INESC TEC*
Porto, Portugal
msjavadi@gmail.com

Rui Castro
*IST* and *INESC-ID*
Lisbon, Portugal
rcastro@tecnico.ulisboa.pt

João P. S. Catalão
*FEUP* and *INESC TEC*
Porto, Portugal
catalao@fe.up.pt

2021 International Conference on Smart Energy Systems and Technologies (SEST) | 978-1-7281-7660-4/21/$31.00 ©2021 IEEE | DOI: 10.1109/SEST50973.2021.9543463

***Abstract*—The trend towards a decentralized, decarbonized, and digital energy system is gaining momentum. A key driver of this change is the rapid penetration increase of Distributed Energy Resources (DER). Commercial consumers can offer significant contributions to future energy systems, especially by engaging in demand response services. Virtual Power Plants (VPP) can aggregate and operate DERs to provide the required energy to the local grid and allowing for the participation in wholesale energy markets. This work considers both the technical constraints of the distribution system as well as the commercial consumer's comfort preferences. A stochastic mixed-integer linear programming (MILP) optimization model is developed to optimize the scheduling of various DERs owned by commercial consumers to maximize the profit of the TVPP. A case study on the IEEE 119-bus test system is carried out. Results from the case study show that the TVPP provides optimal DER scheduling, improved system reliability and increase in demand response engagement, while maintaining commercial consumer comfort levels. In addition, the profit of the TVPP increases by 49.23% relative to the baseline scenario.**

***Keywords*—Consumer comfort, day-ahead energy markets, demand response, energy scheduling, heating ventilation and air conditioning, virtual power plant**

## Nomenclature

### A. Set/indices

| | |
|---|---|
| $s/\Omega^s$ | Index/set of scenarios |
| $h/\Omega^h$ | Index/set of hours |
| $g/\Omega^g$ | Index/set of generators |
| $ev/\Omega^{ev}$ | Index/set of electric vehicles |
| $\varsigma/\Omega^\varsigma$ | Index/set of market |
| $l/\Omega^l$ | Index/set of lines |
| $n,m/\Omega^n$ | Index/set of nodes |
| $k/\Omega^k$ | Index/set of loads |
| $\{r,c,id \in n\}$ | |
| HVAC / $\Omega^{HVAC}$ | Index/set of HVAC system |
| $\omega/\Omega^\omega$ | Index/set of normal operation |

### B. Parameters

| | |
|---|---|
| $g_l, b_l, S_l^{max}$ | Conductance, susceptance, and flow boundaries of each branch $l$ (S, S, MVA) |
| $R_l, X_l$ | Resistance, Reactance (Ω, Ω) |
| $MP_l, MQ_l$ | Big-M parameters related with active and reactive power flows over each branch $l$ |
| $\rho_s$ | Probability of scenario $s$ |
| $OC_g$ | Cost of unit energy production |
| $\lambda_h^{TOU}$ | ToU price associated with customers (€/MWh) |
| $\lambda_h^\varsigma$ | Day-ahead market price (€/MWh) |
| $\lambda_h^{ev}$ | EV discharging cost (€/MWh) |
| $PD_{s,h}^n$ | Demand at node $n$ (MW) |
| $QD_{s,h}^n$ | Reactive demand at node $n$ (MVAr) |
| $V_{nom}$ | Nominal voltage (kV) |
| $\eta_{ev}^{ch}$ | Charging efficiency |
| $\eta_{ev}^{dch}$ | Discharging efficiency |
| $E_{ev,n}^{min}, E_{ev,n}^{max}$ | Energy Storage limit |
| $\mu_{ev}$ | Scaling factor |
| $P_{g,n,s,h}^{DG,min}$, $P_{g,n,s,h}^{DG,max}$ | Power generation limits (MW) |
| $pf_g$ | Power factor of DG's |
| $pf_{ss}$ | Power factor of substation |
| $T_{k,n,s,h}^{ideal}$ | Ideal temperature set-point in house $k$ [°C]. |
| $P_{HVAC,k,n,s,h}^{cool\_max}$ | Actual HVAC unit power consumption of house $k$ in time $h$ |
| $T_{kt0,n,s,h}^{in}$ | Indoor temperature increase for the set-point in house $k$ in period $h$ [°C]. |
| $T_{kt0,n,s,h}^{dec}$ | Indoor temperature decrease concerning the user-selected set-point in house $k$ in period $h$ [°C]. |
| $COP_{HVAC}$ | Coefficient of performance of HVAC in house $k$. |
| $M_k$ | Mass of air in household $k$ [kg]. |
| $c_{air}$ | Thermal capacity of air [kJ/kg·°C].]. |
| $T_{k,n,s,h}^{initial}$ | Initial indoor temperature of household $k$ [°C]. |
| $T_{k,n,s,h}^{Dead-band}$ | Dead-band around the temperature set-point for the HVAC unit of house $k$ [°C]. |
| $T_{kt,n,s,h}^{therm}$ | Thermostat set-point of house $k$ in period h [°C]. |

### C. Variables

| | |
|---|---|
| $P_{\varsigma,n,s,h}^{market}, Q_{\varsigma,s,h}^{market}$ | Power purchased from grid (MW, MVAr) |
| $E_{ev,n,s,h}$ | Reservoir level of EV (MWh) |
| $I_{ev,n,s,h}^{dch}, I_{ev,n,s,h}^{ch}$ | Charging and discharging binary variables |
| $P_{g,n,s,h}^{DG}$, $Q_{g,n,s,h}^{DG}$ | DG power (MW, MVAr) |
| $P_{\varsigma,n,s,h}^{market}$ | Power purchased from market (MW) |
| $P_l, Q_l, \theta_l$ | Active and reactive power flows respectively, and voltage angle difference of branch $l$ (MW, MVAr, radians) |
| $PL_l, PL_l$ | Active and reactive power lines of each branch $l$ (MW, MVAr) |
| $V_{n_i}, V_{n_j}$ | Voltage magnitudes at bus $i$ and $j$ (kV) |
| $u_{l,h}$ | Binary variable representing operating status of DER |
| $\theta_{n_i}, \theta_{n_j}$ | Voltage angle at node $i$ and $j$ (radians) |
| $x_{l,h}$ | Binary variable to indicate line status |
| $y_{l,h}^+, y_{l,h}^-$ | Auxiliary variables to indicate the status of a line |
| $\Delta V_{n,s,h}$ | Voltage deviation magnitude (kV) |
| $\chi_{l,h}$ | Binary switching variable of line $l$ |
| $f_{l,h}$ | Fictitious current flows through line $l$ |
| $g_{n,h}^{SS}$ | Fictitious current injections at substation nodes |
| $d_{n,h}$ | Fictitious nodal demand |
| $n_{DG}$ | Number of candidate nodes for installation of distributed generation |
| $P_{HVAC,k,n,s,h}^{cool}$, $Q_{HVAC,k,n,s,h}^{cool}$ | Active and reactive power flows of HVAC system |
| $T_{(h-1)}^{amb}$ | Ambient temperature in period h in house $k$ [°C]. |

## I. Introduction

Globally, power systems are undergoing a pronounced evolution towards systems that are more decentralized, decarbonized and digital [1]. This shift has seen the emergence of consumer-owned distributed energy resources to become essential features of future power systems [2].

There are many reasons for the emergence of small scale Distributed Energy Resources (DERs) including economic, environmental, energy security, increased resilience and psychological [3], [4]. DERs can provide self-generation for

978-1-7281-7660-4/21/$31.00 ©2021 IEEE

their owner or export excess power to other consumers or the existing electrical grid [5]. The DERs may also offer other services such as flexible generation and demand which can more easily take into account intermittent generation from renewable energy sources (RES) [6]. DERs can also provide important ancillary services to the grid to assist in maintain reserve margins or with issues relating to power quality in the network [7]. New energy markets are emerging that can make use of the potential offered by DERs and new participating agents are also emerging [8].

There exist different categories of consumers, such as commercial, industrial, and residential consumers. Each consumer type has different load profiles, and these profiles may even vary within the consumer type. In the past, DERs have been managed by these individual owners but as the number of these devices has grown, there has emerged the potential for the aggregated control and operation of these devices to operate in energy markets which may have requirements on the minimum bid size to be considered [9].

Recently, the concept of a Virtual Power Plant (VPP) has emerged to help aggregate and coordinate disparate DER devices to participate as a single agent in electricity markets [10]. Typically, VPPs have considered residential consumers in their portfolio but there also exists the possibility of combining different consumer classes into a single VPP to help increase the diversity of its portfolio and maximize the use of various DERs [11]. This diversity introduces the new potential for a VPP but also new challenges associated with meeting requirements related to system operations, reliability, sustainability, economic and environmental objectives while meeting operator and customer demands [12]. Including new consumer types into the VPP operations also introduces new opportunities for active asset manage, such as commercial Heating Ventilation and Air Condition (HVAC) systems which use a major portion of the energy use of commercial buildings and also are a large source of flexible load [12]

Existing VPPs largely focus on the commercial aspect of aggregating DERs for energy market participation. There has been very little research into VPPs that take the technical constraints of the network into account [13]. These VPPs are termed Technical Virtual Power Plants (TVPP). An example of the structure of a TVPP is shown in Fig.1. The figure shows how the TVPP sits at the heart of operations and must communicate with several different agents such as the day-ahead market organizers and the owners of the commercial and residential buildings as well as the inhabitants of these buildings. The TVPP will also need to liaise with renewable energy generators to forecast and estimate supply and demand balances. These supply and demand forecasts will need to be technically feasible and thus, the TVPP is required to oversee the modelling and optimization of the existing network to make sure that the dispatches do not exceed technical constraints and if they do, the TVPP is required to reformulate the internal dispatch order.

The remainder of this paper is structured in the following manner: Section II contains an overview of the current state of the art relating to VPPs. Section III details the methodology followed. The case studies are presented in Section IV as well as the results of the simulations. The conclusions and recommendations for future work are discussed in Section V.

## II. State of the Art

The concept of a Virtual Power plant, an aggregating agent for dispersed DERS so that they can participate in energy markets, has received considerable research interest. Typically, research has focused on maximizing profit or reducing energy losses and has typically only involved residential consumers.

For example, the authors of [14] consider a VPP participating in both energy and regulation services markets using DERs and battery energy storage systems. The model considered residential consumers but did not investigate the potential of commercial or industrial consumers who may have different load profiles and different DERs available.

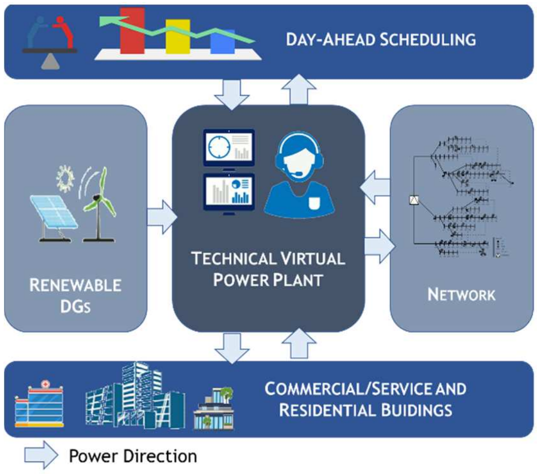

Fig.1:Overview of TVPP concept

Using Electric Vehicles (EVs) as a resource in VPPs was investigated by [15] to help integrate higher levels of wind generation. The authors used a two-stage approach to first design the VPP framework and control method and then in the second stage the optimization of energy storage devices and a coordination strategy for the EVs are presented. The authors did not consider other forms of RES or other types of DERs which may provide additional benefits to the VPP operator, consumers as well as the existing grid operator.

A multi-stage optimization of a VPP considering EVs and demand response programs was conducted by [16]. The authors developed a stochastic mixed-integer linear program to account for uncertainties in the model and used both Time-of-Use (ToU) and Real-Time Pricing tariffs. An interesting aspect of this study is the ability of the VPPs to transact power among themselves to help address technical constraints in the model.

A VPP considering a number of RES generators and commercial loads was developed by [17]. This model was designed to operate in the real-time spot market and use a wide range of the number of participating Distributed Generation (DG) to investigate the effects on operating costs of the VPP. The model did not consider the technical constraints of the grid or the comfort preferences of the consumers.

A two-stage model for VPPs considering RES and thermostatically controlled loads was proposed by [18]. The authors chose HVAC units as the controllable loads and considered both static and dynamic aggregation models. The state model aggregated all the loads at once in the initialization of the model while the dynamic model aggregated the loads at each of the time steps. The model accounted for comfort constraints of the HVAC units but not the technical constraints of the network.

This section has shown that the concept of the VPP has been widely studied considering different aspects however, a research gap has been identified. This is the operation of TVPPs which aggregate commercial DERs and consider various types of uncertainty. Very few papers also consider the technical constraints of the distribution network and simultaneously respect the thermal comfort levels within the commercial buildings. Thus, this paper presents a comprehensive model investigating the potential of a combination of different consumer types, both residential and commercial, to participate in a Day-Ahead Market (DAM) through a TVPP, respecting comfort and grid constraints.

## III. Mathematical Formulation

### A. *Objective Function*

The stochastic model developed in this paper aims to maximize the TVPP's profit from optimally scheduling various DERs from both residential and commercial consumers. This profit is made up of two terms, revenue from power sold to commercial customers (PSC) and the cost of operating the TVPP (TVPPC) plant while considering the technical and economic constraints. This is shown in (1).

$$Max\ \ Profit = PSC - TVPPC \tag{1}$$

The PSC revenue term is decomposed further in (2). This equation represents each consumer's power consumption from daily loads, EV charging and the usage of HVAC systems. The consumer's power consumption is subject to Time of Use (ToU) tariffs.

$$\begin{aligned} PSC = &\sum_{s\in\Omega^s}\rho_s\sum_{h\in\Omega^h}\sum_{k\in\Omega^k}\lambda_h^{TOU}P_{k,s,h} \\ &+\sum_{s\in\Omega^s}\rho_s\sum_{h\in\Omega^h}\sum_{k\in\Omega^k}\sum_{ev\in\Omega^{ev}}\lambda_h^{TOU}P_{ev,k,s,h}^{ch} \\ &+\sum_{s\in\Omega^s}\rho_s\sum_{h\in\Omega^h}\sum_{k\in\Omega^k}\sum_{HVAC\in\Omega^{HVAC}}\lambda_h^{TOU}P_{HVAC,k,s,h}^{cool} \end{aligned} \tag{2}$$

The TVPPC term is shown in (3). These costs include payments to consumer-owned Distributed Generation for electricity produced plus maintenance costs. The revenue from power sold in the day-ahead market and the revenue from the power sold by discharging EVs are subtracted from the TVPPC while a penalty factor is added. The penalty (4) is the price paid to charge EVs or paid to activate the HVAC systems which would not have occurred if the TVPP was not active. In other words, the optimal schedule of the EVs and HVAC units for the owners may be different to the optimal schedule for the TVPP and thus, the TVPP pays for the inconvenience. The normal operating costs are those events that occur in the optimal schedules for both the owner and the TVPP.

$$\begin{aligned} TVPPC = &\sum_{s\in\Omega^s}\rho_s\sum_{h\in\Omega^h}\sum_{k\in\Omega^k}\sum_{g\in\Omega^g}OC_gP_{g,k,s,h}^{DG} \\ &-\sum_{s\in\Omega^s}\rho_s\sum_{h\in\Omega^h}\sum_{k\in\Omega^k}\sum_{\varsigma\in\Omega^\varsigma}\lambda_h^{\varsigma}P_{\varsigma,k,s,h}^{market} \\ &-\sum_{s\in\Omega^s}\rho_s\sum_{h\in\Omega^h}\sum_{k\in\Omega^k}\sum_{ev\in\Omega^{ev}}\lambda_h^{ev}P_{ev,k,s,h}^{dch} \\ &+Penalty \end{aligned} \tag{3}$$

$$Penalty\ = Penalty_{ev} + Penalty\ _{HVAC} \tag{4}$$

$$\begin{aligned} Penalty_{ev} = &\left(\sum_{s\in\Omega^s}\rho_s\sum_{h\in\Omega^h}\sum_{k\in\Omega^k}\sum_{ev\in\Omega^{ev}}P_{ev,k,s,h}^{ch}\lambda_h^{TOU}\right. \\ &\left.-\sum_{s\in\Omega^s}\rho_s\sum_{h\in\Omega^h}\sum_{k\in\Omega^k}\sum_{ev\in\Omega^{ev}}\lambda^{ev}P_{ev,k,s,h}^{dch}\right) \\ &-Cost_{ev,\omega}^{NormalOperation} \end{aligned} \tag{5}$$

$$\begin{aligned} Cost_{ev,\omega}^{NormalOperation} = &\left(\sum_{h\in\Omega^h}\sum_{k\in\Omega^k}\sum_{\omega\in\Omega^\omega}\sum_{ev\in\Omega^{ev}}P_{ev,k,h,\omega}^{ch}\lambda_h^{TOU}\right. \\ &\left.-\sum_{h\in\Omega^h}\sum_{k\in\Omega^k}\sum_{\omega\in\Omega^\omega}\sum_{ev\in\Omega^{ev}}\lambda^{ev}P_{ev,k,h,\omega}^{dch}\right) \end{aligned} \tag{6}$$

$$\begin{aligned} Penalty\ _{HVAC} = &\sum_{s\in\Omega^s}\rho_s\sum_{h\in\Omega^h}\sum_{k\in\Omega^k}\sum_{HVAC\in\Omega^{HVAC}}\lambda_h^{TOU}P_{HVAC,k,s,h}^{cool} \\ &-Cost_{HVAC,\omega}^{NormalOperation} \end{aligned} \tag{7}$$

$$Cost_{HVAC,\omega}^{NormalOperation} = \sum_{h\in\Omega^h}\sum_{k\in\Omega^k}\sum_{\omega\in\Omega^\omega}\sum_{HVAC\in\Omega^{HVAC}}\lambda_h^{TOU}P_{HVAC,k,h,\omega}^{cool} \tag{8}$$

EVs are modelled by the expressions (9)-(14). The maximum charging and discharging rates are governed by (9) and (10) respectively while (11) ensures that charging or discharging cannot occur simultaneously.

$$0 \le P_{ev,k,n,s,h}^{ch} \le I_{ev,k,n,s,h}^{ch}P_{ev,k,n,h}^{ch,max} \tag{9}$$

$$0 \le P_{ev,k,n,s,h}^{dch} \le I_{ev,k,n,s,h}^{dch}P_{ev,k,n,h}^{ch,max} \tag{10}$$

$$I_{ev,k,n,s,h}^{ch} + I_{ev,k,n,s,h}^{ch} \le 1 \tag{11}$$

$$E_{ev,k,n,s,h} = E_{ev,k,n,s,h-1} + \eta_{ev}^{ch}P_{ev,k,n,s,h}^{cg} - \frac{P_{ev,k,n,s,h}^{dch}}{\eta_{ev}^{dch}} \tag{12}$$

$$E_{ev,k,n}^{min} \le E_{ev,k,n,s,h} \le E_{ev,k,n}^{max} \tag{13}$$

$$E_{ev,k,n,s,h0} = \mu_{ev}E_{ev,n}^{max};\ E_{ev,k,n,s,h24} = \mu_{ev}E_{ev,n}^{max} \tag{14}$$

The state of charge (SoC) of the EV is modelled in (12) and relies on the SoC of the previous period plus any additional charging and minus any discharging. Inequality (13) ensures that the storage level is always within a permissible range. Finally, (14) sets the initial storage level and requires that the EV returns to this initial SoC at the end of the operational period. For simplicity, both $\eta_{ev}^{ch}$ and $\eta_{ev}^{dch}$ are set to be equal and are expressed as a percentage, depending on the node where the EVs are connected.

HVAC systems are modelled by expressions (15)-(26) which were obtained from [19]. The temperature limits are set by (15) while (16) bounds the HVAC power use. This model utilizes a thermal resistance model which uses the cooling operation of the HVAC system and is shown in (17). The initial temperature is defined by (18).

Binary operating variables are shown in (19). Maximum and minimum temperature limits are shown in (20) and (21). Equation (22) minimizes the discomfort level of the consumers. Equations (23) and (24) set the upper and lower limits of HVAC operation. The non-negativity constraints for the decision variable are shown in (25) and (26).

$$T_{HVAC,k}^{min} \le T_{k,n,s,h}^{ideal} \le T_{HVAC,k}^{max} \tag{15}$$

$$0 \le P_{HVAC,k,n,s,h}^{cool} \le P_{HVAC,k,n,s,h}^{cool\_max} \tag{16}$$

$$\begin{aligned} T_{kh,n,s,h}^{in} = &\left(1-\frac{\Delta T}{1000\ .\ M_k\ .\ c_{air}\ .\ R_k}\right).T_{k(h-1),n,s,h}^{in} \\ &+\frac{\Delta T}{1000\ .\ M_k\ .\ c_{air}\ .\ R_k}.T_{(h-1)}^{amb} \\ &-\frac{COP_{HVAC}}{0{,}000277\ .\ M_k\ .\ c_{air}}.P_{HVAC,k,n,s,h}^{cool}\ \ ,\ \forall\, k,h>1 \end{aligned} \tag{17}$$

$$T_{kh0,n,s,h}^{in} = T_{k,n,s,h}^{initial}\ ,\forall\, k \tag{18}$$

$$P_{HVAC,k,n,s,h}^{cool} = u_{k,n,s,h}.P_{HVAC,k,n,s,h}^{cool}\ ,\forall\, k,h\ (u = 0\ OFF, u = 1\ ON) \tag{19}$$

$$T_{k,n,s,h}^{in}\ \ \forall\, k,h \in \underset{T_{k,n,s,h}^{inc},T_{k,n,s,h}^{dec},T_{k,n,s,h}^{therm},T_{k,n,s,h}^{in}}{argmin}\left\{\frac{1}{N_k}.\sum_{s\in\Omega^s}\sum_{h\in\Omega^h}\sum_{k\in\Omega^k}\left(T_{k,n,s,h}^{inc}+T_{k,n,s,h}^{dec}\right)\right. \tag{20}$$

subject to:

$$T_{k,n,s,h}^{therm} \le T_{k,n,s,h}^{ideal} + T_{k,n,s,h}^{in}\ ,\forall\, k,h \tag{21}$$

$$-T_{k,n,s,h}^{therm} \le T_{k,n,s,h}^{dec} - T_{k,n,s,h}^{ideal}\ ,\forall\, k,h \tag{22}$$

$$T_{k,n,s,h}^{in} \le T_{k,n,s,h}^{therm} + T_{k,n,s,h}^{Dead-band}\ ,\forall\, k,h \tag{23}$$

$$-T_{k,n,s,h}^{in} \le T_{k,n,s,h}^{Dead-band} - T_{k,n,s,h}^{therm}\ ,\forall\, k,h \tag{24}$$

$$-T_{k,n,s,h}^{dec} \le 0\ ,\forall\, k,h \tag{25}$$

$$\left.-T_{k,n,s,h}^{in} \le 0,\forall\, k,h\ \right\} \tag{26}$$

Kirchhoff's Current law governs the flows of current into and out of a node. This is applied to the active power flow in (27) and the reactive power flows in (28). In these equations $P_{l,s,h}$ and $Q_{l,s,h}$ represent the active and reactive power flow in the line respectively, and $PD_{s,h}^n$ and $QD_{s,h}^n$ represent the active and reactive demand at the nodes, respectively. $PL_{l,s,h}$ and $QL_{l,s,h}$ represent the active and reactive power losses in the line, respectively.

$$\sum_{g\in\Omega^g} P^{DG}_{g,n,s,h} + \sum_{k\in\Omega^k}\sum_{ev\in\Omega^{ev}} \left(P^{dch}_{ev,k,n,s,h} - P^{ch}_{ev,k,n,s,h}\right) + P^{market}_{\varsigma,s,h} + \sum_{in,l\in\Omega^l} P_{l,s,h} - \sum_{out,l\in\Omega^l} P_{l,s,h} = \left(PD^n_{s,h} + P^{cool}_{HVAC,k,n,s,h}\right) + \sum_{in,l\in\Omega^l}\frac{1}{2}PL_{l,s,h} + \sum_{out,l\in\Omega^l}\frac{1}{2}PL_{l,s,h}\,;\ \forall\varsigma\in i \quad (27)$$

$$\sum_{g\in\Omega^g} Q^{DG}_{g,n,s,h} + Q^{market}_{\varsigma,s,h} + \sum_{in,l\in\Omega^l} Q_{l,s,h} - \sum_{out,l\in\Omega^l} Q_{l,s,h} = \left(QD^n_{s,h} + Q^{cool}_{HVAC,k,n,s,h}\right) + \sum_{in.l\in\Omega^l}\frac{1}{2}QL_{l,s,h} + \sum_{out.l\in\Omega^l}\frac{1}{2}QL_{l,s,h}\ \forall\varsigma\in i \quad (28)$$

Inequalities (29) and (30) present linearized AC power flows through each feeder, which are governed by Kirchhoff's Voltage Law. Note that $\theta l,s,h$ refer to the angle difference $\theta n,s,h - \theta m,s,h$ where $n$ and $m$ are bus indices corresponding to the same line $l$, based on [20]. The big-M formulation was used, set to the maximum transfer capacity, to avoid the non-linearity.

$$\left|P_{l,s,h} - (V_{nom}\left(\Delta V_{n,s,h} - \Delta V_{m,s,h}\right)g_k - V^2_{nom}b_k\theta_{l,s,h}\right| \le MP_l \quad (29)$$

$$\left|Q_{l,s,h} - (-V_{nom}\left(\Delta V_{n,s,h} - \Delta V_{m,s,h}\right)b_k - V^2_{nom}g_k\theta_{l,s,h}\right| \le MQ_l \quad (30)$$

The maximum amount of flow that can pass through a line is given by inequality (31). Equations (32) and (33) represent active and reactive power losses in each line *l*.

$$P^2_{l,s,h} + Q^2_{l,s,h} \le \chi_{l,h}(S^{max}_l)^2 \quad (31)$$

$$PL_{l,s,h} = R_l\left(P^2_{l,s,h} + Q^2_{l,s,h}\right)/\,V^2_{nom} \quad (32)$$

$$QL_{l,s,h} = X_l\left(P^2_{l,s,h} + Q^2_{l,s,h}\right)/\,V^2_{nom} \quad (33)$$

The active and reactive power limits of the DGs are given by (34) and (35), respectively. Inequality (36) limits the DGs ability to inject or consume reactive power.

$$P^{DG,min}_{g,n,s,h} \le P^{DG}_{g,n,s,h} \le P^{DG,max}_{g,n,s,h} \quad (34)$$

$$Q^{DG,min}_{g,n,s,h} \le Q^{DG}_{g,n,s,h} \le Q^{DG,max}_{g,n,s,h} \quad (35)$$

$$-\tan\left(cos^{-1}(pf_g)\right)P^{DG}_{g,n,s,h} \le Q^{DG}_{g,n,s,h} \le tan\left(cos^{-1}(pf_g)\right)P^{DG}_{g,n,s,h} \quad (36)$$

For stability reasons, the active and reactive power limits at the substations are given by (37) and (38).

$$P^{market,min}_{\varsigma,s,h} \le P^{market}_{\varsigma,s,h} \le P^{market,max}_{\varsigma,s,h} \quad (37)$$

$$Q^{market,min}_{\varsigma,s,h} \le Q^{market}_{\varsigma,s,h} \le Q^{market,max}_{\varsigma,s,h} \quad (38)$$

The reactive power that is withdrawn from the substation is subject to the bounds presented in inequality (39).

$$-\tan\left(cos^{-1}(pf_\varsigma)\right)P^{market}_{\varsigma,s,h} \le Q^{market}_{\varsigma,s,h} \le tan\left(cos^{-1}(pf_\varsigma)\right)P^{market}_{\varsigma,s,h} \quad (39)$$

Equation (40) requires that all nodes with a demand at hour h are connected and have a single input flow through line l. The inequality shown in (41) places an upper bound of 1 input flow for the terminal nodes.

$$\sum_{l\in\Omega^l}\chi_{l,h} = 1, \forall m\in\Omega^k; l\in n \quad (40)$$

$$\sum_{in.l\in\Omega^l}\chi_{l,h} - \sum_{out.l\in\Omega^l}\chi_{l,h} \le 1, \forall m\notin\Omega^k; l\in n \quad (41)$$

## IV. Case Study, Results and Discussion

In this section, the two main case studies are presented as well as the results of the various simulations. The two case studies consist of a baseline model and a flexible TVPP study. The second case study is further used for three investigations into the effects of different levels of consumer thermal comfort requirements through modifying the HVAC operational limits. The model is programmed in GAMS 24.0 and solved using the CPLEX 12.0 solver. The simulations are conducted on an HP Z820 workstation with two 3.1GHz E5-2687W processors and 256 GB of RAM.

### *A. Case studies*

The standard IEEE-119 bus test system [21] is used to simulate and validate the developed mathematical model. Two types of DG units are considered, namely wind and solar power. For both technologies, the installed capacity of these units is 1 MW. The costs associated with the solar and wind DG units are taken from [22]. The following assumptions and system data are considered in the analysis:

- A time horizon of 24 hours is considered.
- The value assumed for the nominal voltage is 12.66 kV.
- In each node, a voltage deviation of ±5% is considered.
- The reference node is the substation, with a voltage magnitude being set to its nominal value.
- 0.95 is the value of the power factor at the DG units.
- 0.80 is the value of the power factor at the substation.
- Charging and discharging rates for the EVs are the same and equal to 90%
- Charging and discharging costs of the EVs are 5 €/MWh.
- The EVs discharge cannot go below 40% of their total load capacity.
- The operation cost of solar DG units is 40 €/MWh.
- The operation cost of wind DG units is 20 €/MWh.
- Commercial buildings can also charge EVs at night.
- Optimization for usage during a summer period

Commercial customers are distributed throughout the network and are fed through nodes 14, 29, 34, 43, 52, 56, 61, 66, 69, 73, 77, 83, 100, 107, 112 and 116. An HVAC system and an EVs parking lot, containing 10 vehicles, are located at the commercial consumers. The residential consumers are in the remaining nodes and have various DERs. In this model, uncertainty is accounted for by using a set of scenarios. There are three sources of uncertainty, solar generation, wind generation and demand. Three scenarios for each parameter were developed. This resulted in 27 scenarios which were reduced using k means techniques as is described in [20].

Two case studies were considered for this model. Firstly, to establish a baseline for comparing the results of the model, a case study was developed where all the load from the consumers was met through buying power from the DAM market. There were no DG, EVs or flexible HVAC systems used in this case study.

The second case study allows for the TVPP to fully utilize the potential of the DG units to generate electricity, the aggregation of EVs to offer flexible demand and supply through controlled charging and discharging, and flexible HVAC systems in commercial buildings to improve DR flexibility. In this second case study, the consumer comfort requirements are considered in the HVAC system's operation.

The second case study was used to investigate the impacts of various modifications of thermal comfort requirements on the operation of the TVPP. This was done by investigating three different thermal ranges for the commercial buildings. A narrow thermal band limited the indoor temperature to between 20ºC to 22ºC.

A standard band ensured that the indoor temperatures stayed between 19ºC to 23ºC while the wide band maintained the temperatures between 18ºC to 24ºC.

*B. Impact of TVPP on the distribution system*

Table I shows the profit, the power sold to consumers and the TVPP operational cost for both case studies. From the table, it is clear to see that the enhanced operation of the TVPP increases its revenue and decreases costs thus increasing profits. The profit increased by 49.23% relative to the baseline. The PSC revenues are increased by 1.55% relative to the baseline. Therefore, the main driver in the increase in profits is due to decreased TVPPC costs due to the participation of DG.

With the contribution of the DG units and demand response programs to meet the demand, there are a wide diversity of technologies used to meet the scheduled demand. This is shown in Fig. 2 which shows the contribution of each technology in meeting the demand as well as the changing market price throughout the day. Demand Response resources from commercial consumers are initiated during the peak period of 19:00 to 21:00 when the market price is also at its highest. In conjunction with the Demand Response program, the EVs and commercial HVAC systems also contribute to increased system flexibility.

In terms of the energy mix, there is a large contribution from RES, reaching 72.79% of the total demand. Wind generation is the largest contributor supplying 65.61% of demand, however, there is also significant PV generation, especially during its peak production times.

Management of the charging and discharging of the EV fleet is undertaken by the TVPP and the results of this flexible operation are shown in Fig. 3. The charging periods for the EVs occur during periods of low ToU prices. Discharging occurs during working hours and when the ToU price is at its highest during the day. Note that there is discharging between 20:00 to 22:00 despite a lower ToU price. This is due to the high demand and market price during these hours.

A key difference of this TVPP model compared to other VPPs is the consideration of the technical constraints, namely the voltage profile of the system during operation. The voltage profile in each of the case studies is shown in Fig. 4, with Case 1 being the baseline with no TVPP case and case 2 representing the TVPP in operation. The figure shows that there is a significant decrease in the voltage fluctuations experienced by the system in the second case study with the flexible operation of the TVPP.

The deviations are reduced by a maximum of 52.5% between the two cases. The improvements to the voltage profile are due to the presence of the DG units as they generate locally which improves the voltage of the local nodes.

TABLE I: FINANCIAL COMPARISON BETWEEN TWO CASE STUDIES

| | Profit (€) | PSC (€) | TVPP (€) |
|---|---|---|---|
| Baseline | 16 285.80 | 44 091.62 | 28 498.09 |
| TVPP operation | 32 078.58 | 44 783.89 | 12 705.30 |

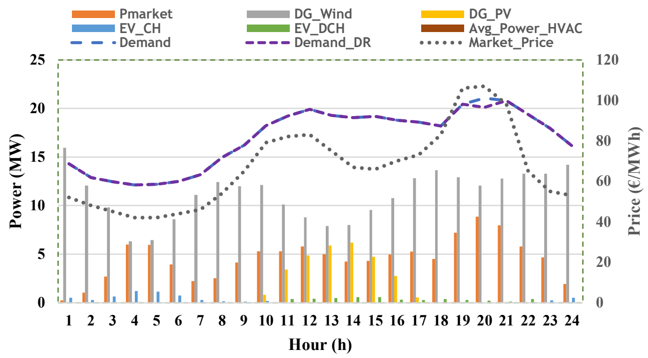


Fig. 2: Energy mix for Case 2

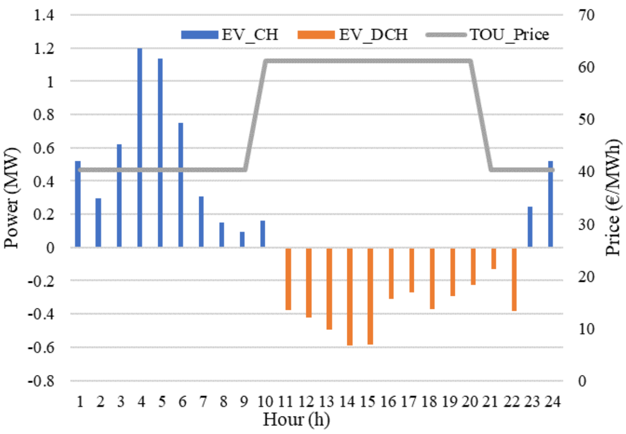


Fig. 3: Charging and discharging profile for the EVs.

The DG units also tend to be located near the end of a line which improves the voltage profile. The largest voltage drops are seen in those nodes located at end nodes of the feeders which can be seen from the grid topology. In addition, the EVs also inject power locally which further improves the voltage profile.

The DGs and EVs combined with the more efficient operation of the HVAC mean that less power is imported from the substation. The improvement in the voltage profile increases system reliability as it can now handle more voltage fluctuations.

*C. Effects on the comfort of commercial consumers*

To investigate the impact of the active management of the HVAC system on the comfort of commercial consumers, three modified case studies were considered. These modified case studies used the flexible TVPP model as the base but modified the acceptable temperature limits for the HVAC system operation in commercial buildings.

In the narrow thermal operating band, due to the stricter operating constraints of the commercial HVAC system, this case study had a lower profit relative to the standard operating model of the TVPP. This was because there was slightly less energy sold by the TVPP combined with an increase in the costs of operating the HVAC units. The higher costs of operation were due to HVAC operation during high energy price periods (especially at 19:00).

In comparison with the standard case, the power used in the narrow operating band scenario is 13.11% higher. These stricter temperature bands did not affect the technical performance of the distribution system as no significant changes occurred to the voltage deviation profile in this case.

The wider thermal operating bands increased the flexibility of the HVAC allowing for an increase in profit by the TVPP. In this case, profits increased by 2.7% relative to the standard case. This profit is driven by a 7.0% reduction in purchasing energy by the TVPP as it can more easily schedule the operation of HVAC units to occur in low-price periods.

The usage of the HVAC system in each of the three case studies (narrow, standard, wide) are shown in Fig. 5. The narrow range case study uses more energy during the day, especially at 18:00 where the ToU cost is high. Thus, there exist clear trade-offs between consumer comfort and savings from the electricity bill. The results in this section have shown the multiple benefits that a TVPP can bring to a distribution system.

Results have shown that there is an increase in the revenues, increase in the amount of locally produced DG generation, increase in the participation of commercial consumers in DR programs, a decrease in the voltage profile, and the comfort of commercial consumers is maintained through intelligent HVAC management.

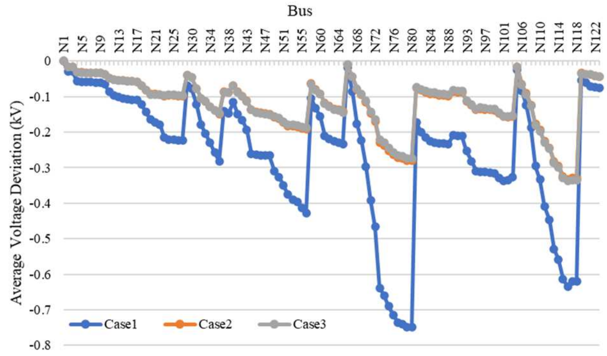


Fig. 4: Comparison of nodal voltages

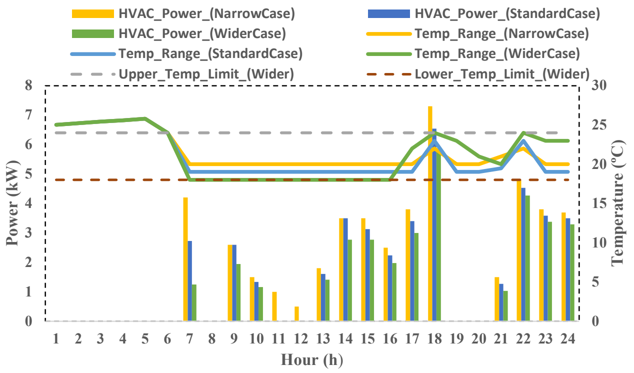


Fig. 5: HVAC power demand from the different cases

## V. Conclusions

This paper has investigated the potential for a TVPP to aggregate DERs, EVs and demand response services from commercial and residential consumers to bid into the DAM market, all the while considering the technical constraints of the distribution system. The TVPP agent aims to optimize the operation of the distribution grid, improve the voltage profile of the system, and increase the financial viability of investing in DERs. This model considered both residential and commercial consumers, each with different DERs and load requirements. The model was tested on two different case studies: one that resembled the current status quo and one where DERs owned by commercial consumers were allowed to participate in the DAM. By utilizing the TVPP as an aggregator of DERs, the profit was increased by 49.23%, PSC revenues increased by 1.55%, RES sources provided 72.79% of total energy demand, the voltage profile of the network was improved by a maximum of 52.5% and all HVAC systems were operated in a way that maintained thermal comfort requirements in the commercial buildings. Different comfort preferences were investigated for the HVAC operation by changing the allowable limits of indoor temperature, which showed a clear trade-off between consumer comfort and cost savings. The improved voltage profiles can help to increase the flexibility, reliability and increase the potential for integration of RES into the distribution network.

## Acknowledgment

J.P.S. Catalão acknowledges the support by FEDER through COMPETE 2020 and FCT, under POCI-01-0145-FEDER-029803 (02/SAICT/2017).

## References

[1] S. Puri, A. T. D. Perera, D. Mauree, S. Coccolo, L. Delannoy, and J.-L. Scartezzini, “The role of distributed energy systems in European energy transition,” *Energy Procedia*, vol. 159, pp. 286–291, Feb. 2019, doi: 10.1016/j.egypro.2019.01.014.

[2] Z. Li, M. Shahidehpour, A. Alabdulwahab, and Y. Al-Turki, “Valuation of distributed energy resources in active distribution networks,” *Electr. J.*, vol. 32, no. 4, pp. 27–36, May 2019, doi: 10.1016/j.tej.2019.03.001.

[3] J. Guerrero, D. Gebbran, S. Mhanna, A. C. Chapman, and G. Verbič, “Towards a transactive energy system for integration of distributed energy resources: Home energy management, distributed optimal power flow, and peer-to-peer energy trading,” *Renew. Sustain. Energy Rev.*, vol. 132, p. 110000, Oct. 2020, doi: 10.1016/j.rser.2020.110000.

[4] B. Parrish, P. Heptonstall, R. Gross, and B. K. Sovacool, “A systematic review of motivations, enablers and barriers for consumer engagement with residential demand response,” *Energy Policy*, vol. 138, p. 111221, Mar. 2020, doi: 10.1016/j.enpol.2019.111221.

[5] B. Zhou *et al.*, “Optimal Coordination of Electric Vehicles for Virtual Power Plants With Dynamic Communication Spectrum Allocation,” *IEEE Trans. Ind. Inform.*, vol. 17, no. 1, pp. 450–462, Jan. 2021, doi: 10.1109/TII.2020.2986883.

[6] Y. Wu, J. Shi, G. J. Lim, L. Fan, and A. Molavi, “Optimal Management of Transactive Distribution Electricity Markets With Co-Optimized Bidirectional Energy and Ancillary Service Exchanges,” *IEEE Trans. Smart Grid*, vol. 11, no. 6, pp. 4650–4661, Nov. 2020, doi: 10.1109/TSG.2020.3003244.

[7] K. Zhang, S. Troitzsch, S. Hanif, and T. Hamacher, “Coordinated Market Design for Peer-to-Peer Energy Trade and Ancillary Services in Distribution Grids,” *IEEE Trans. Smart Grid*, vol. 11, no. 4, pp. 2929--2941, 2020, doi: 10.1109/TSG.2020.2966216.

[8] Z. Yi, Y. Xu, J. Zhou, W. Wu, and H. Sun, “Bi-Level Programming for Optimal Operation of an Active Distribution Network With Multiple Virtual Power Plants,” *IEEE Trans. Sustain. Energy*, vol. 11, no. 4, pp. 2855–2869, Oct. 2020, doi: 10.1109/TSTE.2020.2980317.

[9] A. Rajaei, S. Fattaheian-Dehkordi, M. Fotuhi-Firuzabad, M. Moeini-Aghtaie, and M. Lehtonen, “Developing a Distributed Robust Energy Management Framework for Active Distribution Systems,” *IEEE Trans. Sustain. Energy*, pp. 1–1, 2021, doi: 10.1109/TSTE.2021.3070316.

[10] A. Baringo, L. Baringo, and J. M. Arroyo, “Day-Ahead Self Scheduling of a Virtual Power Plant in Energy and Reserve Electricity Markets under Uncertainty,” *IEEE Trans. Power Syst.*, pp. 1–1, 2018, doi: 10.1109/TPWRS.2018.2883753.

[11] S. Yu, F. Fang, Y. Liu, and J. Liu, “Uncertainties of virtual power plant: Problems and countermeasures,” *Appl. Energy*, vol. 239, pp. 454–470, Apr. 2019, doi: 10.1016/j.apenergy.2019.01.224.

[12] N. Pourghaderi, M. Fotuhi-Firuzabad, M. Moeini-Aghtaie, and M. Kabirifar, “Commercial Demand Response Programs in Bidding of a Technical Virtual Power Plant,” *IEEE Trans. Ind. Inform.*, vol. 14, no. 11, pp. 5100–5111, Nov. 2018, doi: 10.1109/TII.2018.2828039.

[13] K. O. Adu-Kankam and L. M. Camarinha-Matos, “Towards collaborative Virtual Power Plants: Trends and convergence,” *Sustain. Energy Grids Netw.*, vol. 16, pp. 217–230, Dec. 2018, doi: 10.1016/j.segan.2018.08.003.

[14] H. Nguyen-Duc and N. Nguyen-Hong, “A study on the bidding strategy of the Virtual Power Plant in energy and reserve market,” *Energy Rep.*, vol. 6, pp. 622–626, Feb. 2020, doi: 10.1016/j.egyr.2019.11.129.

[15] W. Wang, P. Chen, D. Zeng, and J. Liu, “Electric Vehicle Fleet Integration in a Virtual Power Plant With Large-Scale Wind Power,” *IEEE Trans. Ind. Appl.*, vol. 56, no. 5, pp. 5924–5931, Sep. 2020, doi: 10.1109/TIA.2020.2993529.

[16] F. Sheidaei and A. Ahmarinejad, “Multi-stage stochastic framework for energy management of virtual power plants considering electric vehicles and demand response programs,” *Int. J. Electr. Power Energy Syst.*, vol. 120, p. 106047, Sep. 2020, doi: 10.1016/j.ijepes.2020.106047.

[17] M. Qu, T. Ding, W. Wei, Z. Dong, M. Shahidehpour, and S. Xia, “An Analytical Method for Generation Unit Aggregation in Virtual Power Plants,” *IEEE Trans. Smart Grid*, vol. 11, no. 6, pp. 5466–5469, Nov. 2020, doi: 10.1109/TSG.2020.3002104.

[18] C. Wei *et al.*, “A bi-level scheduling model for virtual power plants with aggregated thermostatically controlled loads and renewable energy,” *Appl. Energy*, vol. 224, pp. 659–670, Aug. 2018, doi: 10.1016/j.apenergy.2018.05.032.

[19] A. Tascikaraoglu, N. G. Paterakis, O. Erdinc, and J. P. S. Catalao, “Combining the Flexibility From Shared Energy Storage Systems and DLC-Based Demand Response of HVAC Units for Distribution System Operation Enhancement,” *IEEE Trans. Sustain. Energy*, vol. 10, no. 1, pp. 137–148, Jan. 2019, doi: 10.1109/TSTE.2018.2828337.

[20] S. F. Santos, D. Z. Fitiwi, M. Shafie-Khah, A. W. Bizuayehu, C. M. P. Cabrita, and J. P. S. Catalao, “New Multistage and Stochastic Mathematical Model for Maximizing RES Hosting Capacity—Part I: Problem Formulation,” *IEEE Trans. Sustain. Energy*, vol. 8, no. 1, pp. 304–319, Jan. 2017, doi: 10.1109/TSTE.2016.2598400.

[21] M. R. M. Cruz, D. Z. Fitiwi, S. F. Santos, and J. P. S. Catalão, “Quantifying the Flexibility by Energy Storage Systems in Distribution Networks with Large-Scale Variable Renewable Energy Sources,” in *2019 IEEE Milan PowerTech*, Jun. 2019, pp. 1–6. doi: 10.1109/PTC.2019.8810952.

[22] S. F. Santos *et al.*, “Impacts of Operational Variability and Uncertainty on Distributed Generation Investment Planning: A Comprehensive Sensitivity Analysis,” *IEEE Trans. Sustain. Energy*, vol. 8, no. 2, pp. 855–869, Apr. 2017, doi: 10.1109/TSTE.2016.2624506.